Conference on Modelling Fluid Flow (CMFF'25)
The 19th International Conference on Fluid Flow Technologies
Budapest, Hungary, August 26-August 29, 2025

Gas Accumulation Behavior in Diverging Channels with Grooves and Bars of Varying Sizes

Michael MANSOUR[1;2], Mena SHENOUDA[3], Nicola ZANINI[4], Dominique THÉVENIN[5],

[1] Corresponding Author. Mechanical Power Engineering Department, Faculty of Engineering - Mataria, Helwan University, 11718 Cairo, Egypt. E-mail: m.botros@m-eng.helwan.edu.eg
[2] Lab. of Fluid Dynamics & Technical Flows, University of Magdeburg "Otto von Guericke", 39106 Magdeburg, Germany. Tel.: +493916758569, Fax: +493916742840, E-mail: michael.mansour@ovgu.de
[3] Lab. of Fluid Dynamics & Technical Flows, University of Magdeburg "Otto von Guericke", 39106 Magdeburg, Germany. E-mail: mena.shenouda@ovgu.de
[4] Department of Engineering - University of Ferrara, Via Saragat 1, 44122, Ferrara, Italy. E-mail: nicola.zanini@unife.it
[5] Lab. of Fluid Dynamics & Technical Flows, University of Magdeburg "Otto von Guericke", 39106 Magdeburg, Germany. E-mail: thevenin@ovgu.de

ABSTRACT

Two-phase flows in diffusers often result in significant gas accumulation due to the presence of low-pressure separation zones, which adversely impacts pressure recovery. This phenomenon limits the performance of centrifugal pumps transporting gas-liquid mixtures. Unlike pumps with rotating components, diffusers offer a simpler setup for precise experimental analysis. This study investigates the effects of geometric modifications on the upper diffuser side, specifically grooves and bars of varying sizes. The goal is to reduce gas accumulation by enhancing turbulence and gas dispersion near the accumulation. A diffuser with an increasing opening angle was used to induce flow separation and gas accumulation. High-speed imaging was employed to capture the two-phase interactions. The results indicate that small-sized grooves and bars have only a limited impact on gas accumulation. In some cases, geometric modifications even intensify flow separation, resulting in a greater gas buildup, especially under low water flow and high air flow conditions. However, larger-sized bars, especially the biggest ones, prove to be most effective in reducing gas accumulation, particularly at higher water flow rates. The outcomes of this research will support the validation of computational models and facilitate design modifications of centrifugal pumps to improve their performance in two-phase flow conditions.

Keywords: Grooves and bars, Turbulent two-phase flow, Gas accumulation, Diverging channels, Diffusers, Centrifugal pumps

NOMENCLATURE

A_u	$[m^2]$	upstream cross-sectional area
D	$[m]$	Depth of groove (or bar)
I	$[cd]$	Light intensity
L_1	$[m]$	upstream straight pipe length
L_2	$[m]$	downstream straight pipe length
Q_G	$[m^3/s]$	gas volume flow rate
Q_L	$[m^3/s]$	liquid volume flow rate
W	$[m]$	Width of groove (or bar)
Re_G	$[-]$	superficial gas Reynolds number
Re_L	$[-]$	superficial liquid Reynolds number
d_{hd}	$[m]$	downstream hydraulic diameter
d_{hu}	$[m]$	upstream hydraulic diameter
p	$[Pa]$	local pressure
p_2	$[Pa]$	reference pressure (sensor 2)
u_G	$[m/s]$	superficial gas velocity
u_L	$[m/s]$	superficial liquid velocity
x	$[m]$	axial distance
y	$[m]$	vertical distance
$\dot{\varepsilon}$	$[\%]$	gas volume fraction
μ_G	$[Pa \cdot s]$	viscosity of gas
μ_L	$[Pa \cdot s]$	viscosity of liquid
ρ_G	$[kg/m^3]$	density of gas

Subscripts and Superscripts

d	downstream
G	gas
h	hydraulic
L	liquid
u	upstream

Abbreviations

% RD	Percentage of reading
LDA	Laser Doppler Anemometry
LED	Light Emitting Diode
LES	Large Eddy Simulation
RSM	Reynolds Stress Model
RTD	Resistance Temperature Detector
VOF	Volume Of Fluid

1. INTRODUCTION

Transporting gas-liquid two-phase mixtures is necessary in various industrial and engineering systems, including pipelines, heat exchangers, nuclear reactors, chemical processing units, solar systems, and oil wells [1–4]. These flows exhibit complex behavior due to the interaction between the two phases, leading to uneven flow patterns and unsteady dynamics. The characteristics of these flows are highly influenced by channel geometry, flow rates, and phase properties, making their prediction and control essential for optimizing system performance and avoiding operational issues such as flow instabilities, pressure fluctuations, and phase separation.

In channels with variable cross-sectional areas, e.g., diverging channels or diffusers, the dynamics of gas-liquid flows become even more intricate. Diverging or expanding cross-sectional areas can lead to significant variations in velocity due to the possibility of flow separation, influencing pressure and void fraction distribution, leading to local gas accumulation [5]. Such large pockets of gas undesirably prevent the diffuser from effectively increasing pressure. Developing techniques to inhibit or decrease gas accumulation in diverging channels is therefore crucial for ensuring effective pressure recovery.

The gas-liquid flow patterns in this expanding channel resemble those in centrifugal pump impellers, where gas buildup causes flow instabilities and reduces pump head and efficiency [6–8]. The complex turbulence and rotational effects in pumps further challenge the accuracy of numerical simulations, especially at high flow rates [5, 9, 10]. Thus, more experiments and improved numerical models are essential for better prediction and control.

This research builds on turbomachinery studies, focusing on how gas buildup in diverging impeller channels degrades centrifugal pump performance. Designed for single-phase flows, these pumps suffer efficiency losses, strong vibrations, flow instabilities, and potential failure when gas accumulates [4, 6, 11, 12]. Understanding gas-liquid interactions is therefore crucial for minimizing gas accumulation and managing two-phase flows effectively.

Researchers have often studied gas-liquid two-phase flow in channels with constant cross-sections to identify flow patterns and measure pressure drops [2, 13, 14]. Similar studies have focused on channels with abrupt cross-sectional changes, like sudden expansions or contractions [2, 15–18]. Other research examined gas-liquid flow in diffusers, such as vertical circular diffusers for pressure recovery [19] and micro-scale converging-diverging rectangular channels for pressure drops [20]. Hwang et al. [20] found that gas velocity decreased in diverging sections, leading to bubble coalescence and significant flow changes. However, most studies used diverging sections with constant opening angles (straight walls) [18–24], which may not fully capture complex flow phenomena like large gas accumulations. The study of two-phase flow in gradually expanding channels with increasing opening angles has received less attention, underscoring the need for further investigation into gas accumulation in these geometries.

A prior study examined two-phase flow regimes in a horizontal, gradually diverging channel [5], identifying key parameters affecting gas accumulation. It was found that large recirculation zones, caused by flow separation, trap gas bubbles, leading to significant accumulations. Increasing the air flow rate resulted in larger accumulations, while increasing the water flow rate initially expanded recirculation zones, increasing accumulation size, until turbulence intensified and reduced the accumulation again. A notable air pocket remained near the end of the diffuser, even at low gas volume fractions (0.05%), negatively affecting velocity distribution and pressure recovery. The study concluded that reducing flow separation or increasing turbulence intensity can help minimize gas accumulation size [5].

The potential of upstream cross-flow steps to reduce gas accumulation in separated turbulent flows was recently explored [25]. These steps enhanced turbulence intensity, breaking larger bubbles into smaller ones and redirecting them towards the channel center, away from the accumulation region. Some step configurations also improved pressure recovery, particularly at higher water flow rates. However, it is important to note that these flow modifications are intrusive elements, affecting inlet conditions.

Several studies [9, 26, 27] validated numerical models against experimental data from [5] to improve prediction accuracy. Kopparthy et al. [9] found that coupling the Reynolds stress model (RSM) with the volume of fluid (VOF) method accurately predicted gas accumulation size and shape, but faced increased errors at high flow. Hundshagen et al. [26] highlighted the impact of turbulence model inaccuracies, noting that the dispersed two-fluid approach sometimes failed to detect gas accumulation. Nguyen et al. [27] achieved the most accurate predictions with a hybrid multiphase model combining Eulerian-Eulerian, VOF, and large eddy simulations (LES), though it was sensitive to prescribed bubble size, requiring further development. These limitations emphasize the continued importance of experimental studies in two-phase flow simulations with significant gas accumulation.

Grooves have been shown to enhance performance and mitigate undesirable phenomena in turbomachinery [28]. In centrifugal compressors, they control rotating stall, though with increased hydraulic losses [29], and in Francis turbine draft tubes, they suppress swirl at the cost of added losses [30, 31]. Grooves have also reduced cavitation in pump inducers [32, 33]. In single-phase centrifugal pumps, micro-grooves on impeller shrouds improve velocity distribution, reduce hydraulic losses, and lessen diffuser separation by smoothing the surface and reducing turbulence [34]. Macro-grooves in mixed

and centrifugal flow pumps reduce inlet swirl, axial thrust, and improve tip leakage flow [35–37]. Additionally, grooved front shrouds in centrifugal pumps enhance secondary flow and improve gas-liquid mixing, reducing gas accumulation [38].

This study investigates the potential to reduce gas accumulation in two-phase flow within a horizontal diverging channel by modifying the upper diffuser wall, where gas typically accumulates. Grooves and bars of various sizes were introduced to enhance turbulence and promote gas dispersion, thus reducing accumulation. The experimental setup and diffuser geometry from previous work [5, 9, 25–27] were retained. A diffuser with a progressively increasing opening angle was used to induce flow separation and gas accumulation. Two-phase flow conditions were varied, with Reynolds numbers for the water and air phases ranging from Re_L = 59530–78330 and Re_G = 3–9.25, respectively. Single-phase flow velocities were measured using Laser Doppler Anemometry (LDA), while high-speed imaging captured two-phase flow dynamics. Some tested designs effectively reduced gas accumulation. The results of this study will be valuable for validating computational models and exploring design modifications for centrifugal pumps operating under two-phase flow conditions, eventually improving their performance.

2. DETAILS OF THE EXPERIMENTS

Figure 1 illustrates the experimental test rig. The diverging section is made of transparent acrylic glass for clear flow observation and optical measurements. A submersible pump circulates water from a 6.0 m^3 tank, while compressed air is introduced through 21 circumferentially arranged 1.0 *mm* holes in a mixing joint. Water and air flow rates are independently measured and regulated using control valves. An electromagnetic flow meter (Endress+Hauser Promag 30F with ± 0.5% RD accuracy) measures water flow, while a rotameter (Yokogawa RGC1263 with ± 2.5% RD accuracy) measures air flow. Two RTD (Resistance Temperature Detector) sensors (Pt100, Class B, ± 0.3 K error) monitor water and air temperatures before mixing. The air supply system includes a service unit, control valve, pressure regulator, and restriction valve for precise control. Eight pressure sensors (Cerabar T PMC131, -1 : $+1$ bar, ± 0.5% RD accuracy) track pressure changes along the diffuser. The estimated average uncertainty in pressure measurements is 2.9% of the reading. Further details on measurement devices can be found in [5, 25].

The flow channel has rectangular cross-sections of 40 × 44 *mm* upstream and 100 × 44 *mm* downstream, yielding a hydraulic diameter ratio of 1.45, with upstream and downstream hydraulic diameters of d_{hu} = 42 *mm* and d_{hd} = 61 *mm*, respectively. The upstream section ($L_1 = 34d_{hu}$) ensures fully developed flow, while the downstream section extends $L_2 = 15.5d_{hu}$. The diffuser features a gradually increasing opening angle to induce flow separation and air accumulation. It starts with a half-included angle of 6°, with the upper curve defined by $x = 13.5y - y^2/10 - 230$ (where x represents the axial direction and y the vertical direction), increasing to 16°. The horizontal flow orientation, while not exactly replicating Coriolis effects in pumps, preserves lateral force interactions, unlike vertical channels where gravity acts parallel to the flow. This setup effectively mimics gas accumulation as observed in impeller channels, enabling investigations into gas accumulation reduction methods.

Single-phase (water) velocity measurements were performed on the upper side of the diffuser using a two-component Laser Doppler Anemometry (LDA) system (Dantec Dynamics 2-D), with an estimated measurement uncertainty below 0.5%. This accounts for statistical (sample size), spatial (grid resolution), and calibration uncertainties. An automatic traversing system acquired velocity data at 325 grid points (10 *mm* horizontal spacing, 7.5 *mm* vertical spacing, see Figure 2a). The velocity was determined from 25,000 samples per point, collected at an average acquisition rate of 1.5 kHz to ensure statistical stability in such turbulent flow. The measurements were performed in the mid-longitudinal section, which provides insights into flow phenomena such as jet direction, flow separation, and turbulence intensity, which are all essential for understanding gas accumulation in two-phase conditions. The precise location of each point was determined through calibration, correcting for laser beam refraction through the acrylic glass and water. Further details about the LDA system and the refraction calibration are available in [39]. Glass spheres with 10 μm mean diameter and 1000 kg/m^3 density were used as tracers. A high-speed camera captured shadowgraphy images, where the channel was backlit by two LED panels positioned opposite the cameras, as shown in Figure 2b). This setup created a dark border at the water-air interface, providing a clear visualization of the size and shape of gas accumulation.

The tested cases involve surface modifications on the upper diffuser wall, specifically three grooves and three bars of varying sizes (Figure 3). The grooves and bars were embedded along the upper wall with the following dimensions (Width, W × Depth, D) 1.0 *mm* × 0.4 *mm* for G1 and B1, 3.0 *mm*× 1.5 *mm* for G2 and B2, and 6.0 *mm*× 3.0 *mm* for G3 and B3. Expressed in dimensionless form relative to the upstream hydraulic diameter (d_{hu}), the corresponding sizes (W/d_{hu}×D/d_{hu}) are 2.4 %×1.0 % for G1 and B1, 7.2 % × 3.6 % for G2 and B2, and 14.3 % × 7.2 % for G3 and B3. These surface structures enhance turbulence and bubble dispersion by introducing localized disturbances along the gas accumulation path. By periodically obstructing the flow, they promote mixing and disturb gas accumulation. The study examines their impact on velocity profiles, gas accumulation, and pressure recovery under single-phase and two-phase flow conditions.

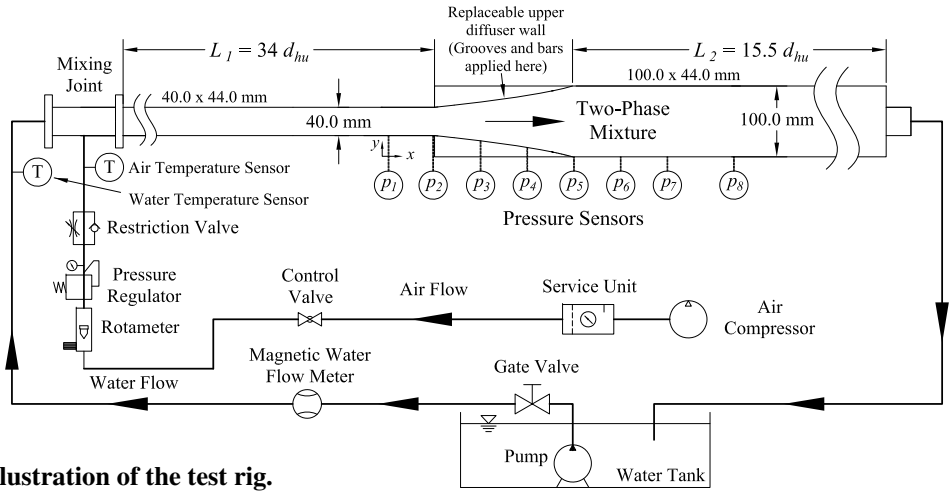

Figure 1. Illustration of the test rig.

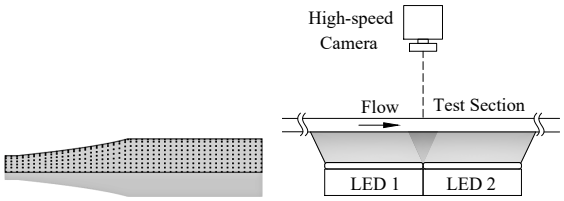

(a) Grid points of LDA **(b) Shadowgraphy top view**

Figure 2. Details of the experiments

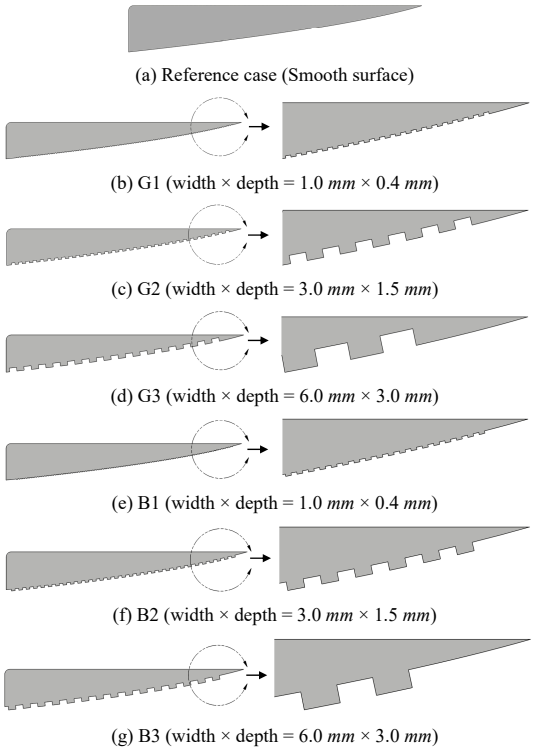

Figure 3. Schematic illustration of diffusers with different artificially introduced grooves and bars.

3. RESULTS

Building on previous studies [5, 9, 26, 27, 39], specific flow conditions were selected to investigate gas accumulation under varying two-phase flow regimes. Two water flow rates (Q_L) and two air flow rates (Q_G) were chosen, resulting in four distinct cases to analyze the influence of different surface modifications. Table 1 summarizes the selected conditions. The superficial Reynolds numbers (Re) for each phase were determined using Eq.1, where ρ represents density, u is the superficial inlet velocity (calculated via Eq.2), μ is dynamic viscosity, and subscripts L and G refer to liquid (water) and gas (air), respectively. The upstream channel cross-sectional area is denoted as A_u. These Reynolds numbers characterize the flow regime of each phase, assuming it occupies the full channel cross-section. The inlet gas volume fraction ($\dot{\varepsilon}$) of each case is determined by by Equation 3. The experimental setup ensured operation under non-cavitating conditions to prevent misinterpretation between air bubbles and vapor cavities. The minimum cavitation number was computed as $\sigma = 18.5$, significantly exceeding the critical threshold ($\sigma_{crit} = 0.3$), even at the maximum velocity, accounting also for flow fluctuations. Consequently, no cavitation was observed during the experiments.

$$\mathrm{Re}_{L,G} = \frac{\rho_{L,G}\, u_{L,G}\, d_{hu}}{\mu_{L,G}} \tag{1}$$

$$u_{L,G} = \frac{Q_{L,G}}{A_u} \tag{2}$$

$$\dot{\varepsilon} = \frac{Q_G}{Q_G + Q_L} \tag{3}$$

Table 1. Flow conditions examined in this study

Case#	Q_L (m^3/s) $\times 10^{-3}$	Q_G (m^3/s) $\times 10^{-6}$	Re_L	Re_G	$\dot{\varepsilon}$ (%)
1	2.64	0	59530	0	0
2	3.47	0	78330	0	0
3	2.64	1.964	59530	3.10	0.074
4	2.64	5.892	59530	9.25	0.223
5	3.47	1.964	78330	3.10	0.056
6	3.47	5.892	78330	9.25	0.169

Figure 4 shows the single-phase velocity magnitudes and fluctuations for all configurations for Case 2. The flow separation increases with groove size due to greater boundary layer disturbance. Similarly, diffusers with bars (B1, B2, B3) exhibit greater flow separation than the smooth reference, with larger bars amplifying velocity fluctuations. Regions of high velocity fluctuations expand as the bar size increases. Further, bars, especially B2 and B3, induce stronger turbulence near the diffuser inlet than grooves, with B3 showing the highest velocity fluctuations, potentially enhancing two-phase mixing.

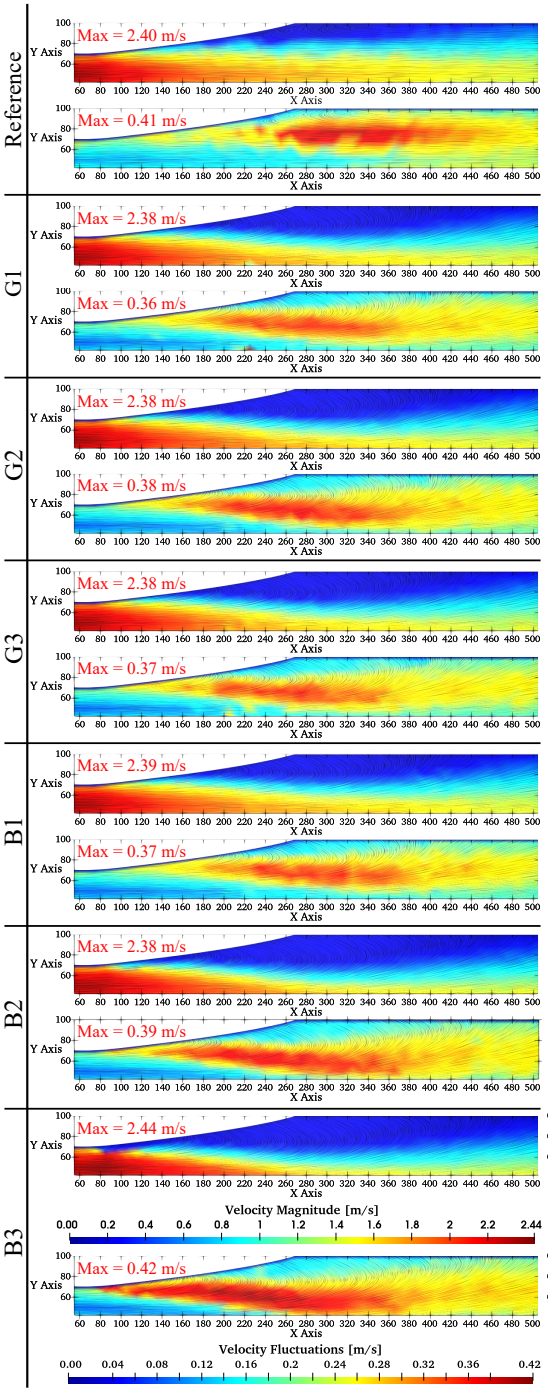

Figure 4. Measured velocities for different configurations (Case 2, Re_L = 78330, Re_G = 0).

Figure 5 illustrates the effects of grooves and bars on gas accumulation in two-phase flow. G1 behaves similarly to the reference case, showing minimal impact of small grooves, while G2 and G3 increase gas accumulation at low water flow, with G3 forming a huge gas cavity in Case 4 due to the increased flow separation. At Re_L = 78330, both G2 and G3 reduce gas buildup by enhancing turbulence and bubble dispersion. Among bars at low flow of water (Re_L = 59530), B1 has little effect, B2 increases accumulation at high gas flow (Case 4), while B3 reduces it in Cases 3 and 4. At Re_L = 78330, B2 and B3 significantly decrease gas accumulation, with B3 performing best across all conditions.

The accumulated air consistently spanned the entire channel width, with minor unsteady variations near the onset of accumulation. To determine the average accumulation size, 1,500 instantaneous images were captured at 50 Hz and processed into a grayscale average image. This stabilized the air-water interface by filtering out transient effects and minimizing potential three-dimensional variations. The grayscale images were then binarized using an intensity threshold (I) derived from their brightness spectra. A MATLAB script automated boundary detection to obtain the accumulation size. Further details on this calculations are available in [5, 39].

Figures 6 and 7 present gas void fraction results, defined as the ratio of mean accumulated gas volume to total channel volume from the diffuser inlet. As shown in Fig. 6, G1 closely follows the reference case, while G2 and G3 increase void fractions at low water flow, with G3 peaking in Case 4. At higher flow, both G2 and G3 reduce gas accumulation, with G3 most effective in Case 5. For bars (Fig. 7), B1 mirrors the reference, B2 increases gas buildup at low water flow (Case 4), and B3 consistently minimizes void fractions, especially at high flow. These findings highlight that G2, G3, B2, and B3 effectively reduce gas accumulation at high liquid velocity, while G1 and B1 provide little improvement. Again, B3 provide improvements for all different conditions. However, the geometry should be carefully selected to control gas accumulation, as the effectiveness varies with flow conditions.

Lastly, Figure 8 shows pressure recovery within the diffuser for all cases, measured at eight axial locations (Fig. 1). To account for turbulence, data were recorded three times at 8 Hz over 15 minutes and averaged. Pressure differences were calculated relative to sensor 2 at the diffuser inlet (x = 0). For the reference case, larger gas accumulations generally reduce pressure recovery. Grooves have little effect at low liquid flow (Re_L = 59530) and worsen recovery at high gas flow (Re_G = 9.25) due to excessive gas buildup. This limited pressure recovery at low liquid flow rates can be attributed to the adverse interaction between the embedded structures (grooves and bars) and the flow dynamics. Specifically, surface structures intensify flow separation along the upper

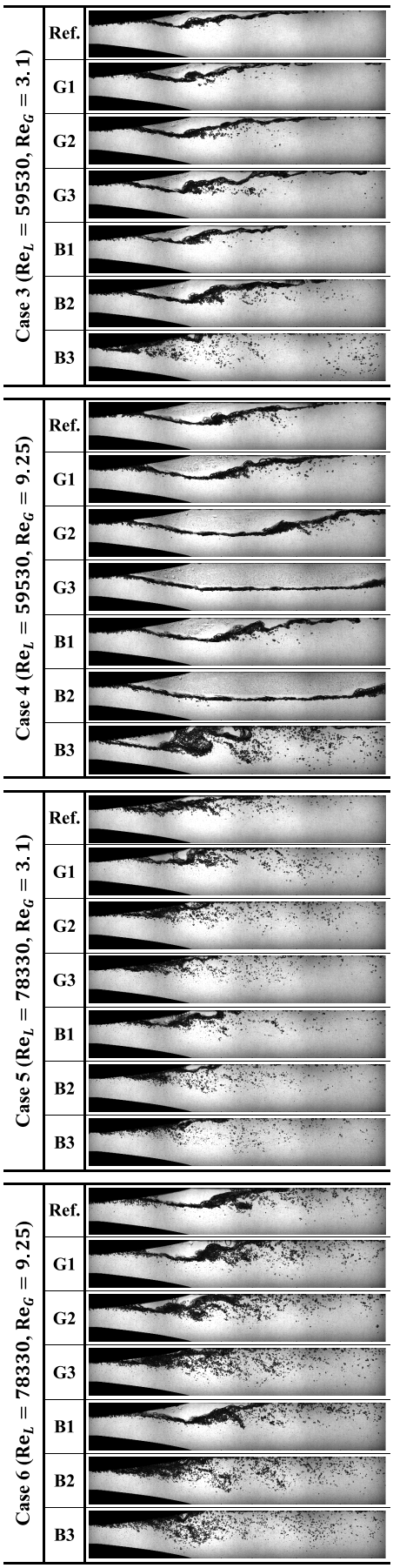

Figure 5. Gas accumulations for different diffusers with grooves and bars.

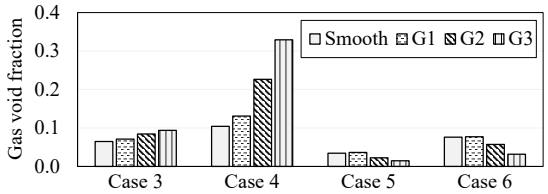

Figure 6. Gas void fractions for different grooves.

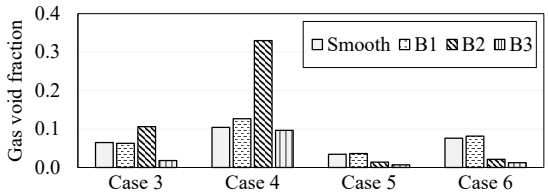

Figure 7. Gas void fractions for different bars.

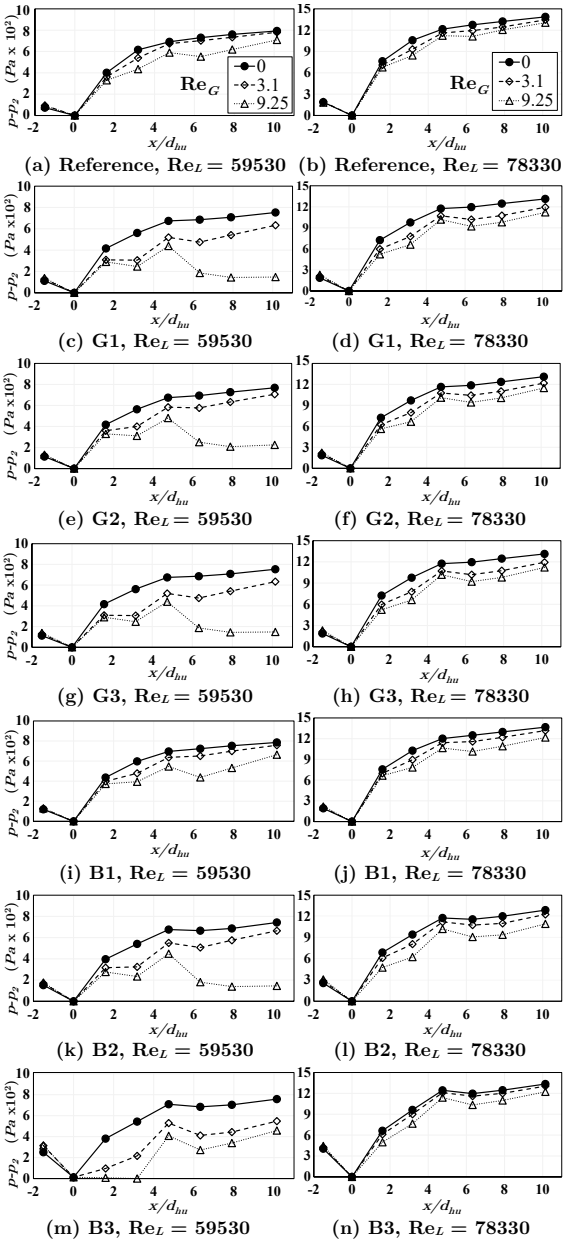

Figure 8. Pressure recovery for all cases (Legend applies to all sub-figures).

wall, which promotes gas accumulation and disrupts the pressure recovery. Furthermore, in the cases of the larger bars (B2 and B3), the reduced inlet cross-sectional area causes flow acceleration, contributing again to reduced pressure recovery. At higher liquid flow, the impact of grooves remains minimal, while all bars closely match the reference case, with B3 offering slight improvement by consistently reducing gas accumulation.

4. CONCLUSIONS

This study examined the effects of surface modifications on the upper diffuser side, specifically grooves and bars of varying sizes, to mitigate gas accumulation in two-phase flow conditions. The findings reveal that small-sized grooves and bars have minimal influence on gas dispersion and, in some cases, exacerbate flow separation, leading to increased gas buildup. Conversely, larger-sized bars, particularly the largest ones, demonstrate significant effectiveness in reducing gas accumulation, especially at higher water flow rates. Pressure recovery is strongly influenced by gas accumulation, with larger accumulations leading to reduced recovery. While grooves have minimal impact, the diffuser with bars, particularly B3, shows a more balanced effect, mitigating gas accumulation while maintaining relatively stable and slightly improved pressure recovery. These insights contribute to a better understanding of two-phase flow behavior in diffusers and provide valuable input for improving computational models and optimizing centrifugal pump designs handling gas-liquid two-phase flows.

ACKNOWLEDGEMENTS

This work is part of a project funded by VDMA (Verband Deutscher Maschinen- und Anlagenbau) and BMWi (Bundesministeriums für Wirtschaft und Energie) under number IGF 23051.

REFERENCES

[1] Ewing, M. E., Weinandy, J. J., and Christensen, R. N., 1999, "Observations of Two-Phase Flow Patterns in a Horizontal Circular Channel", *Heat Transf Eng*, Vol. 20 (1), pp. 9–14.

[2] Chen, I. Y., Tseng, C.-Y., Lin, Y.-T., and Wang, C.-C., 2009, "Two-phase flow pressure change subject to sudden contraction in small rectangular channels", *Int J Multiph Flow*, Vol. 35 (3), pp. 297–306.

[3] Sharma, A., Tyagi, V., Chen, C., and Buddhi, D., 2009, "Review on thermal energy storage with phase change materials and applications", *Renew Sustain Energy Rev*, Vol. 13 (2), pp. 318–345.

[4] Mansour, M., Wunderlich, B., and Thévenin, D., 2018, "Effect of tip clearance gap and inducer on the transport of two-phase air-water flows by centrifugal pumps", *Exp Therm Fluid Sci*, Vol. 99, pp. 487–509.

[5] Mansour, M., Kováts, P., Wunderlich, B., and Thévenin, D., 2018, "Experimental investigations of a two-phase gas/liquid flow in a diverging horizontal channel", *Exp Therm Fluid Sci*, Vol. 93, pp. 210–217.

[6] Mansour, M., Wunderlich, B., and Thévenin, D., 2018, "Experimental study of two-phase air/water flows in a centrifugal pump working with a closed or a semi-open impeller", *ASME Turbo Expo 2018: Turbomachinery Technical Conference and Exposition, Oslo, Norway*, p. V009T27A012.

[7] Mansour, M., Kopparthy, S., and Thévenin, D., 2022, "Investigations on the effect of rotational speed on the transport of air-water two-phase flows by centrifugal pumps", *Int J Heat Fluid Flow*, Vol. 94, p. 108939.

[8] Mansour, M., and Thévenin, D., 2023, "State of the art on two-phase non-miscible liquid/gas flow transport analysis in radial centrifugal pumps Part B: Review of experimental investigations", *Int J Turbomach Propuls Power*, Vol. 8 (4), p. 42.

[9] Kopparthy, S., Mansour, M., Janiga, G., and Thévenin, D., 2020, "Numerical investigations of turbulent single-phase and two-phase flows in a diffuser", *Int J Multiph Flow*, Vol. 130, p. 103333.

[10] Hundshagen, M., Mansour, M., Thévenin, D., and Skoda, R., 2019, "Numerical investigation of two-phase air-water flow in a centrifugal pump with closed or semi-open impeller", *Proceedings of 13th European Turbomachinery Conference on Turbomachinery Fluid Dynamics and Thermodynamics, ETC 2019*.

[11] Zhu, J., Guo, X., Liang, F., and Zhang, H.-Q., 2017, "Experimental study and mechanistic modeling of pressure surging in electrical submersible pump", *J Nat Gas Sci Eng*, Vol. 45, pp. 625–636.

[12] Monte Verde, W., Biazussi, J. L., Sassim, N. A., and Bannwart, A. C., 2017, "Experimental study of gas-liquid two-phase flow patterns within centrifugal pumps impellers", *Exp Therm Fluid Sci*, Vol. 85, pp. 37–51.

[13] Wambsganss, M., Jendrzejczyk, J., France, D., and Obot, N., 1992, "Frictional pressure gradients in two-phase flow in a small horizontal rectangular channel", *Exp Therm Fluid Sci*, Vol. 5 (1), pp. 40–56.

[14] Vallée, C., Höhne, T., Prasser, H.-M., and Sühnel, T., 2008, "Experimental investigation and CFD simulation of horizontal stratified two-phase flow phenomena", *Nucl Eng Des*, Vol. 238 (3), pp. 637–646.

[15] Chen, I. Y., Liu, C.-C., Chien, K.-H., and Wang, C.-C., 2007, "Two-phase flow characteristics across sudden expansion in small rectangular channels", *Exp Therm Fluid Sci*, Vol. 32 (2), pp. 696–706.

[16] Abdelall, F. F., Hahn, G., Ghiaasiaan, S. M., Abdel-Khalik, S. I., Jeter, S. S., Yoda, M., and Sadowski, D. L., 2005, "Pressure drop caused by abrupt flow area changes in small channels", *Exp Therm Fluid Sci*, Vol. 29 (4), pp. 425–434.

[17] Ahmed, W. H., Ching, C. Y., and Shoukri, M., 2008, "Development of two-phase flow downstream of a horizontal sudden expansion", *Int J Heat Fluid Flow*, Vol. 29 (1), pp. 194–206.

[18] Pakhomov, M. A., and Terekhov, V. I., 2022, "Modeling of turbulent heat-transfer augmentation in gas-droplet non-boiling flow in diverging and converging axisymmetric ducts with sudden expansion", *Energies*, Vol. 15 (16).

[19] Anupriya, S., and Jayanti, S., 2014, "Experimental and modelling studies of gas–liquid vertical annular flow through a diverging section", *Int J Multiph Flow*, Vol. 67, pp. 180–190.

[20] Hwang, J. J., Tseng, F. G., and Pan, C., 2005, "Ethanol-CO_2 two-phase flow in diverging and converging microchannels", *Int J Multiph flow*, Vol. 31 (5), pp. 548–570.

[21] Deniz, E., and Eskin, N., 2015, "Hydrodynamic characteristics of two-phase flow through horizontal pipe having smooth expansion", *ISI Bilim Ve Tek Dergisi-Journal Therm Sci Technol*, Vol. 35 (1), pp. 1–9.

[22] Kourakos, V. G., Rambaud, P., Chabane, S., Pierrat, D., and Buchlin, J. M., 2009, "Two-phase flow modelling within expansion and contraction singularities", *Comput Methods Multiph Flow V*, Vol. 63, p. 27.

[23] Eskin, N., and Deniz, E., 2012, "Pressure Drop of Two-Phase Flow through Horizontal Channel with Smooth Expansion", *Int. Refrig. Air Cond. Conf.*, pp. 1–10.

[24] Ahmadpour, A., Noori Rahim Abadi, S., and Kouhikamali, R., 2016, "Numerical simulation of two-phase gas–liquid flow through gradual expansions/contractions", *Int J Multiph Flow*, Vol. 79, pp. 31–49.

[25] Mansour, M., Zanini, N., Shenouda, M., Pinelli, M., Suman, A., and Thévenin, D., 2025, "Minimizing gas accumulation in two-phase flow within a diverging horizontal channel using cross-flow millimeter-size steps", *Proceedings of 16th European Turbomachinery Conference on Turbomachinery Fluid Dynamics and Thermodynamics, ETC16, Hannover, Germany*.

[26] Hundshagen, M., Mansour, M., Thévenin, D., and Skoda, R., 2021, "3D simulation of gas-laden liquid flows in centrifugal pumps and the assessment of two-fluid CFD methods", *Exp Comput Multiph Flow*, Vol. 3 (3), pp. 186–207.

[27] Nguyen, B.-D., Popp, S., Hundshagen, M., Skoda, R., Mansour, M., Thévenin, D., and Hasse, C., 2022, "Large eddy simulations of turbulent gas-liquid flows in a diverging horizontal channel using a hybrid multiphase approach", *J Fluids Eng*, Vol. 145 (3), p. 031501.

[28] Kurokawa, J., 2011, "J-groove technique for suppressing various anomalous flow phenomena in turbomachines", *Int J Fluid Mach Syst*, Vol. 4 (1), pp. 1–13.

[29] Kurokawa, J., Saha, S. L., Matsui, J., and Kitahora, T., 2000, "Passive control of rotating stall in a parallel-wall vaneless diffuser by radial grooves", *J Fluids Eng*, Vol. 122 (1), pp. 90–96.

[30] Chen, Z., Singh, P. M., and Choi, Y.-D., 2017, "Suppression of unsteady swirl flow in the draft tube of a Francis hydro turbine model using J-Groove", *J Mech Sci Technol*, Vol. 31 (12), pp. 5813–5820.

[31] Chen, Z., Baek, S.-H., Cho, H., and Choi, Y.-D., 2019, "Optimal design of J-groove shape on the suppression of unsteady flow in the Francis turbine draft tube.", *J Mech Sci Technol*, Vol. 33 (5).

[32] Choi, Y.-D., Kurokawa, J., and Imamura, H., 2007, "Suppression of Cavitation in Inducers by J-Grooves", *J Fluids Eng*, Vol. 129 (1), pp. 15–22.

[33] Shimiya, N., Fujii, A., Horiguchi, H., Uchiumi, M., Kurokawa, J., and Tsujimoto, Y., 2008, "Suppression of cavitation instabilities in an inducer by j groove", *J Fluids Eng*, Vol. 130 (2).

[34] Skrzypacz, J., and Bieganowski, M., 2018, "The influence of micro grooves on the parameters of the centrifugal pump impeller", *Int J Mech Sci*, Vol. 144, pp. 827–835.

[35] Saha, S. L., Kurokawa, J., Matsui, J., and Imamura, H., 2000, "Suppression of performance curve instability of a mixed flow pump by use of J-groove", *J Fluids Eng*, Vol. 122 (3), pp. 592–597.

[36] Shimura, T., Kawasaki, S., Uchiumi, M., and Matsui, J., 2011, "Internal flow and axial thrust balancing of a rocket pump", *Fluids Engineering Division Summer Meeting*, Vol. 44403, pp. 145–152.

[37] Khoeini, D., and Shirani, E., 2019, "Influences of Diffuser Vanes Parameters and Impeller Micro Grooves Depth on the Vertically Suspended Centrifugal Pump Performance", *J Mech*, Vol. 35 (5), pp. 735–746.

[38] Mansour, M., Kopparthy, S. B., and Thévenin, D., 2023, "Improving air-water two-phase flow pumping in centrifugal pumps using novel grooved front shrouds", *Chem Eng Res Des*, Vol. 197, pp. 173–191.

[39] Mansour, M., 2020, "Transport of two-phase air-water flows in radial centrifugal pumps", Ph.D. thesis, University of Magdeburg, Germany.